

Kinetics and Thermodynamics of Alkene Complexation in d⁰ Metal–Alkyl–Alkene Complexes

Charles P. Casey,* Jennifer Fisher Klein, and Maureen A. Fagan

Contribution from the Department of Chemistry, University of Wisconsin, Madison, Wisconsin 53706

Received August 26, 1999

Abstract: Alkene dissociation from the yttrium chelate Cp*₂Y[η¹,η²-CH₂CH₂CH₂CH=CH₂] (**7-on**) became slow enough below -100 °C to be measured by dynamic ¹H NMR spectroscopy [ΔG[‡](-110 °C) = 7.5 kcal mol⁻¹, ΔH[‡] = 9.3 kcal mol⁻¹]. Coalescence of the Cp* resonances of Cp*₂Y[η¹,η²-CH₂CH₂CH(CH₃)CH=CH₂] (**8-on**) requires alkene dissociation plus inversion at yttrium and occurred substantially slower than simple alkene dissociation [ΔG[‡](-72 °C) = 9.6 kcal mol⁻¹, ΔH[‡] = 10.8 kcal mol⁻¹]. The binding energy of a disubstituted alkene to a d⁰ yttrium center was determined to be ΔH^o = 2.6 kcal mol⁻¹ by direct observation of the equilibrium between Cp*₂Y(η¹,η²-CH₂CH₂CH₂C(CH₃)=CH₂) (**6-on**) and Cp*₂Y(η¹-CH₂CH₂CH₂C(CH₃)=CH₂) (**6-off**). The significantly greater ΔH[‡] of alkene dissociation compared with ΔH^o of alkene binding can be attributed either to stabilization of the dissociated yttrium alkyl by a β-agostic interaction or to destabilization of the transition state leading to alkene dissociation by increased strain in the chelate tether. Binding energies of monosubstituted alkenes were determined indirectly by comparing the relative binding energies of 2,5-dimethyl-THF to both **6** and monosubstituted alkene chelates. Binding energies of monosubstituted alkenes were found to be greater than for disubstituted alkenes; for Cp*₂Y(η¹,η²-CH₂CH₂CH₂CH=CH₂) (**7-on**), ΔH^o = 4.0 kcal mol⁻¹. The rate of alkene dissociation from these yttrium chelates is much faster than reversible intramolecular insertion of the coordinated alkene into the metal alkyl bond to produce cyclobutylmethylmetal compounds.

Introduction

d⁰ metal–alkyl–alkene complexes have been proposed as key intermediates in Ziegler–Natta alkene polymerization (Scheme 1).¹ The Cossee–Arlman mechanism features a simple metal–alkyl–alkene intermediate, while the modified proposals of Brookhart, Green, and Rooney include an additional α-agostic interaction in the alkyl group.² However, there has been no direct observation of a d⁰ metal–alkyl–alkene complex in an active polymerization system.³ This is attributed to very weak binding of alkenes to d⁰ metals incapable of back-bonding to the alkene and to the very rapid insertion of alkene into a metal alkyl bond.

Recently, we reported the synthesis and characterization of Cp*₂Y[η¹,η²-CH₂CH₂C(CH₃)₂CH=CH₂] (**1**), the first d⁰ metal–alkyl–alkene complex. In this case, complexation is favored by chelation and alkene insertion is disfavored by the strain of the cyclobutylmethyl yttrium insertion product. Other recently reported d⁰ metal–alkene complexes stabilized by chelation include Jordan's zirconium–alkoxy–alkene complex **2**,⁴ Royo's

zirconium–alkyl–alkene complex **3**,⁵ Erker's complex **4**,⁶ which has an additional Zr–C–B interaction, and our zirconium–alkyl–alkene chelate **5**⁷ (Scheme 2).

Here we report the first detailed thermodynamic and kinetic studies of d⁰ metal–alkyl–alkene complexes. We have found that alkene dissociation from yttrium chelates such as **1** can be slowed to measurable rates below -100 °C, and we have measured activation barriers for alkene dissociation. We have directly measured the binding energy of a disubstituted alkene to yttrium in the chelate complex Cp*₂YCH₂CH₂CH₂C(CH₃)=CH₂ (**6**) by observing the equilibrium constant between chelated and free alkene species. By measuring the relative binding energies of 2,5-dimethyl-THF to both **6** and monosubstituted alkene chelates, we have indirectly determined the binding energy of monosubstituted alkenes to yttrium. We have also obtained activation barriers for alkene dissociation plus inversion at yttrium; inversion of configuration at metal centers is important in controlling the stereochemistry of formation of syndiotactic polypropylene. The rate of alkene dissociation from these yttrium chelates is much faster than reversible intramolecular insertion of the coordinated alkene into the metal alkyl bond. The binding energies of the alkenes to d⁰ yttrium in this system suggest that observation of a d⁰ ytrocene–alkyl–alkene complex in which the alkene is not tethered to another ligand is entirely possible.

(1) Reviews: (a) Kaminsky, W.; Arndt, M. *Adv. Polym. Sci.* **1997**, *127*, 143. (b) Bochmann, M. *J. Chem. Soc., Dalton Trans.* **1996**, 255. (c) Brintzinger, H. H.; Fischer, D.; Mülhaupt, R.; Rieger, B.; Waymouth, R. M. *Angew. Chem., Int. Ed. Engl.* **1995**, *34*, 1143.

(2) (a) Arlman, E. J.; Cossee, P. *J. Catal.* **1964**, *3*, 99. (b) Brookhart, M.; Green, M. L. H.; Wong, L.-L. *Prog. Inorg. Chem.* **1988**, *36*, 1. (c) Brookhart, M.; Green, M. L. H. *J. Organomet. Chem.* **1983**, *250*, 395. (d) Dawoodi, Z.; Green, M. L. H.; Mtetwa, V. S. B.; Prout, K. *J. Chem. Soc., Chem. Commun.* **1982**, 1410. (e) Ivin, K. J.; Rooney, J. J.; Stewart, C. D.; Green, M. L. H.; Mahtab, R. *J. Chem. Soc., Chem. Commun.* **1978**, 604.

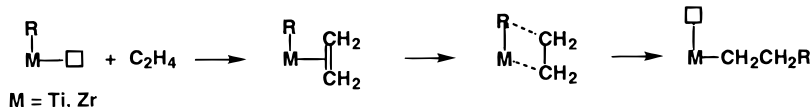
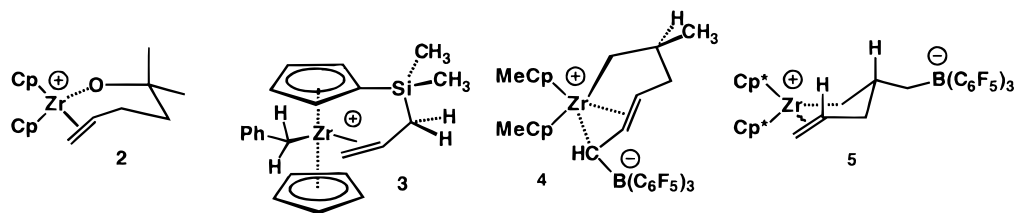
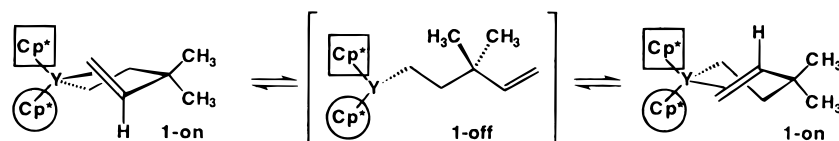
(3) d⁸ palladium– and d⁶ cobalt–alkyl–alkene complexes have been directly observed in olefin polymerizations involving late transition metals. (a) Rix, F. C.; Brookhart, M. *J. Am. Chem. Soc.* **1995**, *117*, 1137. (b) Brookhart, M.; Volpe, A. F. Jr.; Lincoln, D. M.; Horváth, I. T.; Millar, J. M. *J. Am. Chem. Soc.* **1990**, *112*, 5634.

(4) Wu, Z.; Jordan, R. F.; Petersen, J. L. *J. Am. Chem. Soc.* **1995**, *117*, 5867–5868.

(5) Galakhov, M. V.; Heinz, G.; Royo, P. *Chem. Commun.* **1998**, 17.

(6) Karl, J.; Dahlmann, M.; Erker, G.; Bergander, K. *J. Am. Chem. Soc.* **1998**, *120*, 5643.

(7) Casey, C. P.; Carpenetti, D. W.; Sakurai, H., *J. Am. Chem. Soc.* **1999**, *121*, 9483.

Scheme 1. Cossee–Arlman Mechanism for Ziegler–Natta Alkene Polymerization**Scheme 2****Scheme 3****Results**

The preparation of d^0 yttrium chelate complex $\text{Cp}^*_2\text{Y}[\eta^1, \eta^2\text{-CH}_2\text{CH}_2\text{C}(\text{CH}_3)_2\text{CH}=\text{CH}_2]$ (**1**) from the yttrium hydride dimer $(\text{Cp}^*\text{YH})_2$ and 3,3-dimethyl-1,4-pentadiene at -78°C was reported recently.⁸ Evidence for a chelated structure was derived from changes in the ^1H and ^{13}C NMR chemical shifts upon coordination, reversal of these changes upon displacement of the alkene by THF, and observation of nOe effects between Cp^* methyl protons and vinyl hydrogens. Quantitative analysis of the ^1H NOESY time course with the conformer population analysis method demonstrated that in solution chelate complex **1** exists as a twist-boat conformer. According to molecular mechanics calculations, the twist-boat conformation is 3.5 kcal mol $^{-1}$ more stable than its chair counterpart, which has an unfavorable axial methyl to Cp^* steric interaction.

Kinetics of Alkene Dissociation from Metal–Alkyl–Alkene Complexes. Complex **1** has two diastereotopic Cp^* ligands, and a static chelated structure should possess two inequivalent Cp^* NMR resonances. The troubling observation of only a single Cp^* resonance for **1** in both ^1H and ^{13}C NMR spectra at -100°C in methylcyclohexane- d_{14} forced us to propose equilibration of the Cp^* ligands via rapid dissociation of the alkene followed by recomplexation to the opposite alkene enantioface (Scheme 3). We attempted to slow averaging of the Cp^* ligands, but NMR spectroscopy at temperatures below -100°C was restricted by deteriorating line shapes due to the increasing viscosity of methylcyclohexane- d_{14} . Pentane- d_{12} is less viscous and has a slightly lower freezing point than methylcyclohexane- d_{14} , but did not dissolve yttrium chelate complex **1**. Changing to a 1:1 mixture of methylcyclohexane- d_{14} /pentane- d_{12} permitted us to observe **1** between -140 and -100°C .

Two inequivalent Cp^* methyl resonances appeared at δ 11.7 and 11.6 in the ^{13}C NMR spectrum of **1** at -126°C in methylcyclohexane- d_{14} /pentane- d_{12} (Figure 1). These resonances broadened upon warming to -116°C , coalesced at -110°C , and sharpened to a singlet at -101°C .⁹ Line shape analysis of the Cp^* methyl resonances in ^{13}C NMR spectra between -126

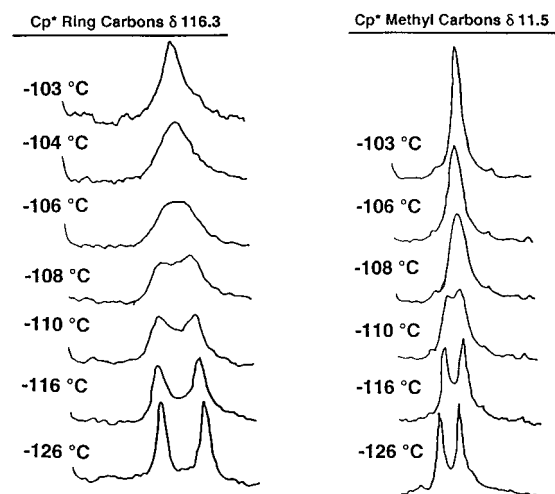


Figure 1. Variable-temperature ^{13}C NMR spectra of $\text{Cp}^*_2\text{Y}[\eta^1, \eta^2\text{-CH}_2\text{CH}_2\text{C}(\text{CH}_3)_2\text{CH}=\text{CH}_2]$ (**1**) in methylcyclohexane- d_{14} /pentane- d_{12} .

and -106°C using the WinDNMR program¹⁰ gave $\Delta G^\ddagger(-110^\circ\text{C}) = 8.2 \pm 0.2$ kcal mol $^{-1}$, $\Delta H^\ddagger = 10.2 \pm 0.4$ kcal mol $^{-1}$, and $\Delta S^\ddagger = 12 \pm 2$ eu for Cp^* exchange. The observation of two inequivalent Cp^* ligands confirms the structure of **1** as a chelate which undergoes rapid and reversible dissociation of the pendant alkene.

$\text{Cp}^*_2\text{Y}[\eta^1, \eta^2\text{-CH}_2\text{CH}_2\text{CH}_2\text{CH}=\text{CH}_2]$ (**7**) and $\text{Cp}^*_2\text{Y}[\eta^1, \eta^2\text{-CH}_2\text{CH}_2\text{CH}_2\text{C}(\text{CH}_3)=\text{CH}_2]$ (**6**) showed similar dynamic behavior in their low-temperature NMR spectra, corroborating a chelated structure for these d^0 yttrium–alkyl–alkene complexes. The ^{13}C NMR spectrum of **7** at -130°C had two Cp^* methyl resonances at δ 12.0 and 11.4 which coalesced on warming to -110°C .¹¹ Spectra between -125 and -102°C were simu-

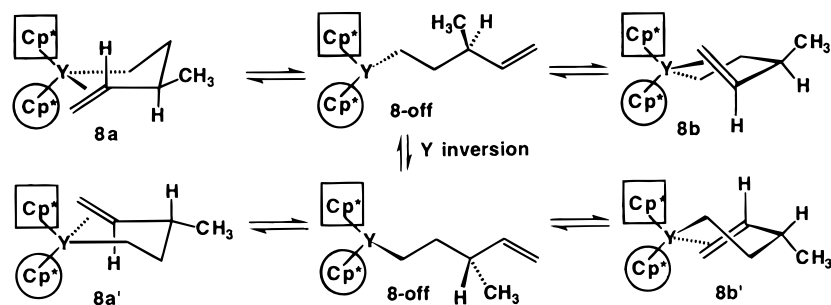
(9) At -126°C , the Cp^* ring carbon ^{13}C NMR signals were separated (δ 116.4, 116.1). These resonances broadened at -116°C and coalesced at -108°C [$\Delta G^\ddagger(-108^\circ\text{C}) = 8.2 \pm 0.2$ kcal mol $^{-1}$, $\Delta H^\ddagger = 10.9 \pm 0.6$ kcal mol $^{-1}$, $\Delta S^\ddagger = 16 \pm 4$ eu]. The two diastereotopic *gem*-methyl groups were indistinguishable by ^{13}C NMR spectroscopy at -112°C , though the methyl resonance at δ 43.1 was broad ($\Delta\omega_{1/2} = 44$ Hz).

(10) Reich, H. J. *J. Chem. Educ.* **1995**, *72*, 1086.

(11) The ^{13}C NMR signal for the Cp^* ring carbons was broad (δ 116.2, $\Delta\omega_{1/2} = 11.2$ Hz) at -130°C , but the two Cp^* resonances did not decoalesce. The Cp^* methyl resonances also broadened without separation in the ^1H NMR spectrum at -130°C (δ 1.92, $\Delta\omega_{1/2} = 15.0$ Hz, Cp^*CH_3).

(8) (a) Casey, C. P.; Hallenbeck, S. L.; Wright, J. M.; Landis, C. R. *J. Am. Chem. Soc.* **1997**, *119*, 9680. (b) Casey, C. P.; Hallenbeck, S. L.; Pollock, D. W.; Landis, C. R. *J. Am. Chem. Soc.* **1995**, *117*, 9770.

Scheme 4



lated using the WinDNMR program to give $\Delta G^\ddagger(-110^\circ\text{C}) = 7.5 \pm 0.2 \text{ kcal mol}^{-1}$, $\Delta H^\ddagger = 9.3 \pm 0.3 \text{ kcal mol}^{-1}$, and $\Delta S^\ddagger = 11 \pm 2 \text{ eu}$. The disubstituted alkene of chelate **6** reversibly dissociated at a rate similar to monosubstituted alkenes of chelates **1** and **7**. Two separate Cp* resonances (δ 1.93, 1.88) were visible only in the ^1H NMR spectrum of **6** at -142°C . Coalescence occurred at -123°C . Simulated spectra between -133 and -120°C gave $\Delta G^\ddagger(-123^\circ\text{C}) = 7.5 \pm 0.2 \text{ kcal mol}^{-1}$, $\Delta H^\ddagger = 10.9 \pm 0.3 \text{ kcal mol}^{-1}$, and $\Delta S^\ddagger = 23 \pm 9 \text{ eu}$. The positive entropies measured for the equilibration of the Cp* ligands for complexes **1**, **6**, and **7** are consistent with an intramolecular process in which the pendant alkene is released from the metal center.

Kinetics of Inversion at Yttrium. We have previously reported the variable-temperature ^{13}C NMR spectroscopy of $\text{Cp}^*_2\text{YCH}_2\text{CH}_2\text{CH}(\text{CH}_3)\text{CH}=\text{CH}_2$ (**8**) in 1:1 methylcyclohexane- d_{14} /pentane- d_{12} .¹² Chelate **8** has two stereocenters: the enantioface of the alkene and the γ -methine carbon on the chelate backbone. The two diastereomers, **8a** (tether methyl cis to the internal vinyl hydrogen) and **8b** (tether methyl trans to the internal vinyl hydrogen), are interconverted by alkene dissociation followed by recomplexation to the opposite alkene enantioface without inversion at the yttrium center. Both **8a** and **8b** possess a pair of diastereotopic Cp* ligands which are exchanged by alkene dissociation followed by inversion at the metal center and recomplexation. This is illustrated in Scheme 4 by the equilibrium between **8a** and **8a'** (or **8b** and **8b'**). This process interchanges the positions of the Cp* ligands relative to both the internal vinyl hydrogen and the tether methyl.

By analogy to complexes **1**, **6**, and **7**, diastereomers **8a** and **8b** should be in slow equilibrium on the NMR time scale below -100°C and two pairs of diastereotopic Cp* ligands are expected to appear in ^{13}C NMR spectra. Surprisingly, only one pair of Cp* ligands was visible in the ^{13}C NMR spectrum of **8** at -128°C , with two sharp Cp* methyl resonances at δ 12.0 and 11.5 and ring carbon resonances at δ 116.2 and 116.1. Further cooling to -142°C failed to reveal a second set of Cp* resonances. Since only a single diastereomer was seen and the detection limit for a second isomer is $\sim 5\%$, the ^{13}C NMR spectra indicate that one diastereomer is favored by a factor ≥ 19 . At temperatures above -100°C , where alkene dissociation is fast, **8a** and **8b** are presumably in rapid equilibrium that is largely biased toward one diastereomer.

The Cp* methyl resonances of **8** broadened on warming to -90°C and coalesced at -72°C . Simulated spectra between -62 and -86°C provided kinetic parameters for Cp* exchange, $\Delta G^\ddagger(-72^\circ\text{C}) = 9.6 \pm 0.3 \text{ kcal mol}^{-1}$, $\Delta H^\ddagger = 10.8 \pm 0.5 \text{ kcal mol}^{-1}$, and $\Delta S^\ddagger = 5.3 \pm 2.7 \text{ eu}$.¹³ The activation energy for Cp* exchange is 2 kcal mol^{-1} greater than the average of

activation energies measured for interchange of Cp* groups in chelate complexes **1**, **6**, and **7**. The Cp* ligands of **8** are exchanged not simply by alkene dissociation and recomplexation to the opposite face but by alkene dissociation coupled with inversion at yttrium, a combined process that interconverts the two diastereotopic Cp* rings of the favored diastereomer.

Molecular mechanics calculations suggest that **8a** adopts a chair conformation with an equatorial methyl group that is $1.5 \text{ kcal mol}^{-1}$ more stable than **8b**, which is held in a twist-boat conformation to avoid an unfavorable axial methyl to Cp* steric interaction.¹² ^1H NMR coupling constants support the proposed chair conformation. ^1H and ^{89}Y decoupled spectra of **8** at 0°C provided coupling constants for each alkyl hydrogen along the chelate backbone. The coupling of the γ -methine hydrogen (δ 2.04) to the β - YCH_2CH at δ 1.45 is 12.5 Hz, indicating that both of these hydrogens are axial. A smaller axial-equatorial coupling is observed between the γ -methine hydrogen and the β - YCH_2CH at δ 1.97, $^3J_{\text{HH}} = 4.0 \text{ Hz}$. The α - YCH at δ -0.89 is held in an axial position ($^3J_{\text{axial-axial}} = 12.5 \text{ Hz}$, $^3J_{\text{axial-equatorial}} = 7.5 \text{ Hz}$) while the α - YCH at δ 0.28 showed coupling to the neighboring β - YCH_2CH_2 typical of an equatorial hydrogen ($^3J_{\text{equatorial-axial}} = 5.0 \text{ Hz}$, $^3J_{\text{equatorial-equatorial}} = 3.6 \text{ Hz}$).

Alkene Coordination Equilibria of Chelated Metal-Alkyl-Alkene Complexes. For yttrium-alkyl-alkene complexes **1**, **7**, and **8**, in which a monosubstituted alkene is coordinated to the metal, little or no temperature dependence of the chemical shifts of the terminal alkene or α -methylene hydrogen resonances was observed between -50 and -100°C . For example, for $\text{Cp}^*_2\text{Y}(\eta^1, \eta^2\text{-CH}_2\text{CH}_2\text{C}(\text{CH}_3)_2\text{CH}=\text{CH}_2)$ (**1**), the chemical shift of the internal vinyl hydrogen (H_{in}) shifted only 0.02 ppm between -100°C (δ 6.78) and -50°C (δ 6.76), and the chemical shifts of the terminal vinyl hydrogens shifted only 0.07 and 0.01 ppm between -100°C (δ 3.76 and 5.14) and -50°C (δ 3.83 and 5.13). This was taken as evidence that the alkene remained fully coordinated to the metal throughout the temperature range.

In contrast, there was a pronounced temperature dependence of the chemical shifts of the α - CH_2 and the alkene hydrogen resonances of the disubstituted alkene chelate $\text{Cp}^*_2\text{YCH}_2\text{CH}_2\text{CH}_2\text{C}(\text{CH}_3)=\text{CH}_2$ (**6**) (Scheme 5, Figure 2). We attribute these spectral changes to a temperature-dependent equilibrium between chelated (**6-on**) and nonchelated (**6-off**) complexes. The observation of a significant amount of **6-off** indicates that the chelate is destabilized by steric crowding between the Cp* methyl groups and the methyl group on the alkene.

At -137°C , the major species present is **6-on** and alkene dissociation is slow on the NMR time scale. Two equal intensity

(13) The Cp* ring carbon NMR resonances of **8** broadened at -90°C and coalesced at -81°C ($\Delta G^\ddagger(-81^\circ\text{C}) = 9.8 \pm 0.5 \text{ kcal mol}^{-1}$). The Cp* methyl hydrogens were visible at δ 1.92 and 1.91 in the ^1H NMR spectrum at -118°C . Coalescence occurred at -90°C ($\Delta G^\ddagger(-90^\circ\text{C}) = 9.7 \pm 0.4 \text{ kcal mol}^{-1}$).

(12) Casey, C. P.; Fagan, M. A.; Hallenbeck, S. L. *Organometallics* **1998**, *17*, 287.

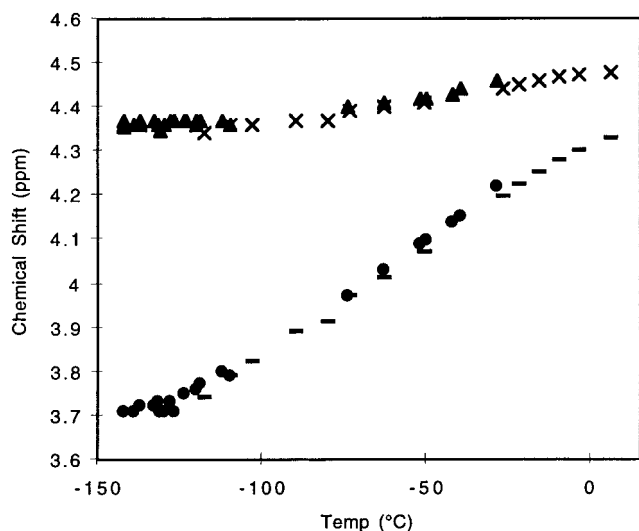
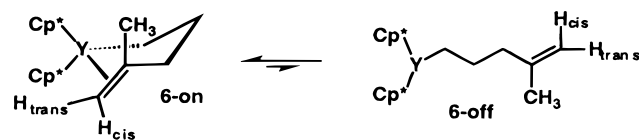


Figure 2. Temperature dependence of the ^1H NMR chemical shifts of the vinyl protons of the disubstituted alkene chelate **6**: (●) H_{trans} in 1:1 methylcyclohexane- d_{14} /pentane- d_{12} ; (—) H_{trans} in methylcyclohexane- d_{14} ; (▲) H_{cis} in 1:1 methylcyclohexane- d_{14} /pentane- d_{12} ; (×) H_{cis} in methylcyclohexane- d_{14} .¹⁶

Scheme 5



resonances were seen for the diastereotopic Cp^* groups of **6** at δ 1.87 and 1.93, and the terminal alkene resonances plateaued at δ 3.71 (H_{trans}) and δ 4.36 (H_{cis}).¹⁴ The chemical shift difference between the terminal alkene hydrogen resonances, $\Delta\delta(=\text{CH}_2)$, in the chelate **6-on** was 0.650 ppm.

The chemical shift difference between the terminal alkene hydrogens for the nonchelated isomer **6-off** was estimated using models. For the THF complex $\text{Cp}^*_2\text{Y}[\eta^1\text{-CH}_2\text{CH}_2\text{CH}_2\text{C}(\text{CH}_3)=\text{CH}_2](\text{THF})$ (**9**),¹⁵ the difference in the chemical shift of the alkene protons was 0.030 ppm, and for the starting diene ($\text{CH}_2=\text{CHCH}_2\text{C}(\text{CH}_3)=\text{CH}_2$) the difference in chemical shift was also 0.030 ppm. With excellent estimates of $\Delta\delta(=\text{CH}_2)$ for both **6-on** and **6-off**, the relative amounts present at a given temperature were estimated from the difference in the alkene hydrogen chemical shifts of the equilibrating mixture at that temperature using eq 1, where x is the mole fraction of **6-on**.

$$\Delta\delta(=\text{CH}_2) = x(0.650) + (1 - x)(0.030) \quad (1)$$

At the lowest temperatures, the major species is **6-on** and $\Delta\delta(=\text{CH}_2)$ is large (Table 1). As the temperature is raised to -51 °C, about half of the alkene is coordinated. At the highest temperatures, the major species is **6-off**. The free energy difference between bound and free alkene in this system containing a disubstituted alkene is very small. At -103 °C, for example, chelation is favored by $0.5 \text{ kcal mol}^{-1}$, while at 6 °C chelation is disfavored by $0.8 \text{ kcal mol}^{-1}$.

For the equilibrium between **6-on** and **6-off**, ΔH° is especially significant because it is the binding energy of the disubstituted alkene in this system, and it is a value that can be extrapolated

(14) In contrast to chelate **1**, in which one terminal vinyl hydrogen resonance shifts to higher frequency and the other shifts to lower frequency, both of the vinyl hydrogen resonances of chelate **6** shift to lower frequency.

(15) See Supporting Information.

Table 1. $\Delta\delta(=\text{CH}_2)$, % **6-on**, K_{Eq} , and ΔG for the Equilibrium between **6-on** and **6-off**

temp (°C)	$\Delta\delta(=\text{CH}_2)$ (ppm $\times 10^3$)	% 6-on	% 6-off	K_{eq}	ΔG (kcal mol^{-1})
6	150	20	80	4.02	-0.8
-27	240	34	66	1.92	-0.3
-51	340	50	49	0.99	0
-63	390	58	42	0.74	0.1
-103	540	83	17	0.21	0.5

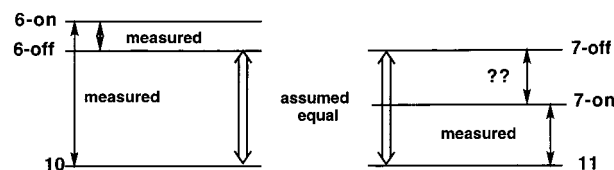


Figure 3. Estimation of free energy of alkene coordination in **7-on** is determined from relative free energies of 2,5-dimethyl-THF complexation to **6-on** and **7-on**, absolute measurement of free energy of alkene coordination in **6-on**, and assumption that energies of complexation of 2,5-dimethyl-THF to **6-off** and **7-off** are equal.

to nonchelating systems. A van't Hoff plot gave $\Delta H^\circ = 2.6 \pm 0.1 \text{ kcal/mol}$ and $\Delta S^\circ = 12 \pm 1 \text{ eu}$ for decomplexation of the alkene in **6**.¹⁵

Relative Binding Constants of 2,5-Dimethyl-THF to Mono- and Disubstituted Alkene Chelates. Little or no temperature dependence is observed in the vinyl chemical shifts of monosubstituted alkene chelates **1**, **7**, and **8** from -50 to -140 °C. This indicates that only chelates are present. Consequently, equilibrium constants between bound and free monosubstituted alkenes cannot be directly measured.

Since these monosubstituted alkene chelates are more closely related to propene and other terminal alkenes used in industrial polymerizations, we have sought indirect means of determining their binding energies. To determine how much more tightly the terminal alkene ligands of **1**, **7**, and **8** bind than the disubstituted alkene of **6**, we needed to find a ligand that would partially displace the alkene ligands. Measurement of the relative magnitude of the equilibrium constants permits quantitative estimates of the greater binding energy of terminal alkenes. Fortunately, it was found that 2,5-dimethyl-THF partially displaces both the monosubstituted and the disubstituted tethered alkenes.

This method conceptually breaks down the 2,5-dimethyl-THF complexation into two separate processes, an equilibrium between chelate and a noncoordinated complex, and 2,5-dimethyl-THF complexation to the noncoordinated compound. It relies on the assumption that 2,5-dimethyl-THF binds equally well to either **6-off** or **7-off**. This is reasonable since the presence or absence of a methyl group on the noncoordinated alkene should have little effect on the ability of the complex to coordinate 2,5-dimethyl-THF. The difference in the free energy of 2,5-dimethyl-THF coordination to monosubstituted chelate complex **7-on** and to disubstituted chelate **6-on** should also be the free energy difference between mono- and disubstituted alkene binding. Since the free energy difference of alkene binding to **6-on** was directly measured, the free energy of binding to **7-on** can be obtained (Figure 3).

High concentrations of 2,5-dimethyl-THF (0.20 M, 8.5 equiv) completely displaced the coordinated alkene of **6** and produced the 2,5-dimethyl-THF adduct, $\text{Cp}^*_2\text{Y}[\eta^1\text{-CH}_2\text{CH}_2\text{CH}_2\text{C}(\text{CH}_3)=\text{CH}_2](2,5\text{-dimethyl-THF})$ (**10**). Vinyl hydrogen resonances of **10** appear at δ 4.57 and 4.54 at -80 °C ($\Delta\delta(=\text{CH}_2) = 0.030$

Table 2. $\Delta\delta(=\text{CH}_2)$, Concentrations of the Components in the Equilibrium between **6-on**, **6-off**, and **10**, Equilibrium Constants, and Free Energy Difference

temp (°C)	$\Delta\delta(=\text{CH}_2)$ (ppm $\times 10^3$)	[6-on] ^a $\times 10^3$ M	[nonchelate] ^a $\times 10^3$ M	[6-off] ^b $\times 10^3$ M	[10] ^c $\times 10^3$ M	[2,5-dimethyl-THF] ^d	temp (°C)	K_{eq}	ΔG (kcal mol ⁻¹)
-65	34	0.20	31	0.14	31	0.046	-65		
-55	44	0.70	31	0.62	30	0.047	-55	900	-2.9
-45	64	1.7	29	1.9	27	0.049	-45	340	-2.6
-42	75	2.2	29	2.8	26	0.050	-42	220	-2.5
-36	85	2.7	28	3.9	24	0.051	-36	170	-2.4
-33	100	3.4	27	5.4	22	0.053	-33	120	-2.3

^a Calculated from $\Delta\delta$ between vinyl hydrogens and eq 1. ^b Calculated from [**6-on**] and K_{eq} for the equilibrium between **6-on** and **6-off**. ^c [**10**] is the difference between [total nonchelate] and [**6-off**]. ^d [2,5-Dimethyl-THF] is the difference between total 2,5-dimethyl-THF (0.077 M) and [**10**].

Table 3. Summary of ΔG° , ΔG_{236} ,¹⁹ ΔH° , and ΔS° for the Equilibria between Mono- and Disubstituted Chelates and 2,5-Dimethyl-THF-Bound Species

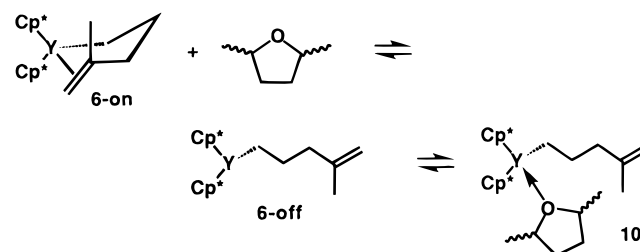
compd	ΔG° (kcal mol ⁻¹)	ΔG_{236} (kcal mol ⁻¹)	ΔH° (kcal mol ⁻¹)	ΔS° (eu)
6-on \rightleftharpoons 10	-0.9 \pm 0.5	-2.5 \pm 0.1	-9.2 \pm 0.5	-28 \pm 3
7-on \rightleftharpoons 11	1.7 \pm 1.1	-0.3 \pm 0.2	-7.8 \pm 1.1	-32 \pm 5
8-on \rightleftharpoons 12	1.3 \pm 1.0	-0.3 \pm 0.2	-6.7 \pm 1.0	-27 \pm 3
1-on \rightleftharpoons 13	0.6 \pm 0.5	-1.1 \pm 0.1	-8.6 \pm 0.5	-31 \pm 2

ppm).¹⁷ No temperature dependence of the vinyl hydrogen resonances was seen between -80 and -10 °C, signifying that **10** is the only species present.

At lower concentrations of 2,5-dimethyl-THF, the pendant disubstituted alkene competes with the bulky 2,5-dimethyl-THF for coordination at yttrium, and three yttrium species are present: **6-on**, **6-off**, and **10**. Addition of 2,5-dimethyl-THF (0.077 M, 2.5 equiv) to a solution of **6** (0.031 M) altered the chemical shift difference between the terminal vinyl hydrogens of **6**. At all temperatures, $\Delta\delta(=\text{CH}_2)$ is smaller in the presence of 2,5-dimethyl-THF due to displacement of the coordinated alkene. At -64 °C, the alkene is almost completely displaced from yttrium and $\Delta\delta(=\text{CH}_2) = 0.034$ ppm; in the absence of 2,5-dimethyl-THF at -63 °C, $\Delta\delta(=\text{CH}_2)$ is 0.386 ppm, corresponding to 58% **6-on**. As the temperature is raised to -45 °C, $\Delta\delta(=\text{CH}_2)$ increases to 0.064 ppm, consistent with the presence of 5% **6-on**; in the absence of 2,5-dimethyl-THF at -51 °C, $\Delta\delta(=\text{CH}_2)$ is 0.340 ppm, corresponding to 50% **6-on**.¹⁸ At -33 °C, $\Delta\delta(=\text{CH}_2)$ is 0.100 ppm (11% **6-on**), and at -27 °C, $\Delta\delta(=\text{CH}_2)$ is 0.240 ppm (34% **6-on**). At temperatures above -33 °C, **6** began to decompose, and data above this temperature was found to be unreliable.

Calculating equilibrium constants for the equilibrium between **6-on** and **10** was complicated by the presence of temperature dependent amounts of **6-off**. The concentration of **6-on** and the total concentration of the two nonchelating species, **6-off** and **10**, were determined from measurements of $\Delta\delta(=\text{CH}_2)$ as described earlier. [**6-off**] was determined from [**6-on**] and the

measured equilibrium constant for **6-off**:**6-on**. The concentration of 2,5-dimethyl-THF complex **10** was determined by subtracting [**6-off**] from the total concentration of noncoordinated species. Finally, the concentration of free 2,5-dimethyl-THF was calculated as the difference between the total concentration of 2,5-dimethyl-THF and [**10**]. Table 2 lists $\Delta\delta(=\text{CH}_2)$, concentrations of species, equilibrium constants, and free energy differences. A van't Hoff plot¹⁵ was used to estimate ΔG° , ΔH° , and ΔS° (Table 3).



Addition of 2,5-dimethyl-THF to solutions of monosubstituted alkene chelates **1**, **7**, and **8** produced large changes in the ¹H NMR chemical shifts of the alkene hydrogens. The vinyl hydrogen chemical shifts showed a pronounced temperature dependence. This is consistent with partial displacement of the chelated alkene by 2,5-dimethyl-THF and with a temperature dependence of the equilibrium constant.

Addition of a high concentration of 2,5-dimethyl-THF (0.14 M) to a solution of Cp*₂Y(η^1 , η^2 -CH₂CH₂CH₂CH=CH₂) (**7**) (0.028 M) at -85 °C led to complete displacement of the chelated alkene by 2,5-dimethyl-THF and formation of Cp*₂Y(η^1 -CH₂CH₂CH₂CH=CH₂)(2,5-dimethyl-THF) (**11**). The chemical shifts for the vinyl protons of **11** [δ 5.79 (H_{int}), 4.85 (H_{cis}), and 4.77 (H_{trans})] were greatly shifted from those of chelate **7** [δ 6.58 (H_{int}), 5.25 (H_{cis}), and 3.79 (H_{trans})]. Significantly, $\Delta\delta(\text{H}_{\text{int}} - \text{H}_{\text{trans}}) = 2.79$ ppm for **7** was reduced to $\Delta\delta(\text{H}_{\text{int}} - \text{H}_{\text{trans}}) = 1.02$ for 2,5-dimethyl-THF complex **11**.²⁰ As the sample was warmed to -67 °C, $\Delta\delta(\text{H}_{\text{int}} - \text{H}_{\text{trans}})$ increased to 1.50 ppm. The warmest temperature at which a ¹H NMR spectrum of this sample was obtained was -37 °C, and at this temperature $\Delta\delta(\text{H}_{\text{int}} - \text{H}_{\text{trans}})$ was 2.32 ppm.

To calculate the fractions of **7** that were chelated and nonchelated in the presence of 2,5-dimethyl-THF, a method similar to that used for the disubstituted alkene was employed. In the absence of 2,5-dimethyl-THF, **7** is 100% chelated and $\Delta\delta(\text{H}_{\text{int}} - \text{H}_{\text{trans}}) = 2.79$ ppm. In the THF-bound complex, Cp*₂Y(η^1 -CH₂CH₂CH₂CH=CH₂)(THF) (**14**), the alkene is not chelated at all and $\Delta\delta(\text{H}_{\text{int}} - \text{H}_{\text{trans}}) = 0.98$ ppm. The fractions

(19) At -37 °C (236 K), we have excellent direct measurement of the equilibria between **7-on** and **11**. For equilibria between **6-on** and **10**, **6-on** and **6-off**, **7-on** and **11**, **8-on** and **12**, and **1-on** and **13**, data was obtained at temperatures below and above -37 °C and free energy and equilibrium constants can easily be interpolated to -37 °C.

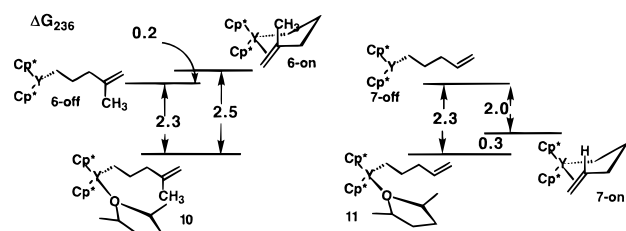
(16) Chemical shifts of the vinyl hydrogens were virtually identical in either methylcyclohexane-*d*₁₄ or 1:1 methylcyclohexane-*d*₁₄/pentane-*d*₁₂.

(17) 2,5-Dimethyl-THF is purchased from Aldrich as a 1:1 mixture of *cis* and *trans* isomers, and both isomers bind equally well to the Cp*₂Y-alkyl complexes. For example, the ¹H NMR spectrum of Cp*₂Y(η^1 -CH₂CH₂CH₂CH=CH₂)(2,5-dimethyl-THF) (**11**) at -122 °C shows approximately equal resonances for the α -CH₂ protons of complexed *cis*- and *trans*-2,5-dimethyl-THF (Figure 18, Supporting Information). At -80 °C, two broad ¹H NMR resonances appear at δ 3.78 ($\Delta\omega_{1/2} = 28$ Hz) and δ 4.01 ($\Delta\omega_{1/2} = 28$ Hz) for rapidly exchanging bound and free *cis*-2,5-dimethyl-THF and for rapidly exchanging bound and free *trans*-2,5-dimethyl-THF.

(18) At higher temperatures, 2,5-dimethyl-THF binds to yttrium less well because the formation of the bimolecular complex is entropically disfavored. Intramolecular coordination of the tethered alkene is less entropically disfavored and competes with 2,5-dimethyl-THF for complexation at yttrium more effectively at higher temperature.

Table 4. K_{Eq} and ΔG for Equilibria between Monosubstituted Alkene Chelates and 2,5-Dimethyl-THF-Bound Species

temp (°C)	compd	K_{eq} (M^{-1})	ΔG
-60	7	11	-1.0
-51	7	5.5	-0.8
-49	7	3.9	-0.6
-42	7	3.3	-0.5
-37	7	2.0	-0.3
-58	8	10	-1
-53	8	5.4	-0.7
-47	8	3.4	-0.6
-24	8	1.1	0
-64	1	106	-1.9
-51	1	37	-1.6
-41	1	16	-1.3
-32	1	9.1	-1.1

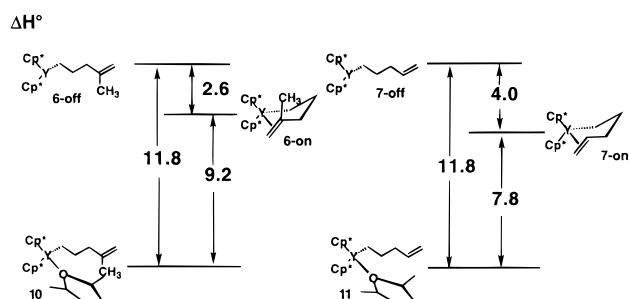
**Figure 4.** Free energy diagrams for monosubstituted and disubstituted alkene chelates and their nonchelated and 2,5-dimethyl-THF-bound forms.

of chelated **7-on** and of nonchelated **7-off** were calculated from the observed $\Delta\delta(\text{H}_{\text{int}}-\text{H}_{\text{trans}})$ using eq 2, where x = the fraction chelated. Calculation of the equilibrium constant was straightforward since only two yttrium species, **7-on** and **11**, are present. Similar procedures were used to measure equilibrium constants for binding of 2,5-dimethyl-THF to monosubstituted alkene chelates **1** and **8**. Data for all three compounds are summarized in Table 4. van't Hoff plots¹⁵ were used to estimate ΔG° , ΔH° , and ΔS° (Table 3).

$$\Delta\delta = x(2.79) + (1 - x)(0.98) \quad (2)$$

At -37°C , K_{eq} for the equilibrium between **7-on** and **11** is 2.0 M^{-1} , which is 98 times smaller than the analogous equilibrium constant for the disubstituted chelate **6-on** and **10**. The free energy difference for 2,5-dimethyl-THF displacement of the monosubstituted chelate **7-on** ($-0.3 \text{ kcal mol}^{-1}$) is $2.2 \text{ kcal mol}^{-1}$ smaller than the free energy difference for displacement of the disubstituted chelate **6-on** ($-2.5 \text{ kcal mol}^{-1}$). As pointed out above, this is also the free energy difference between

(20) At -85°C , broad ^1H resonances appear at δ 3.85 ($\Delta\omega_{1/2} = 51 \text{ Hz}$) and δ 4.06 ($\Delta\omega_{1/2} = 65 \text{ Hz}$) for rapidly exchanging bound and free *cis*- and *trans*-2,5-dimethyl-THF. At -122°C , five resonances are seen for the α -hydrogens of THF, corresponding to decoalesced resonances for both free and bound 2,5-dimethyl-THF. The resonances for free *cis*-2,5-dimethyl-THF and for free *trans*-2,5-dimethyl-THF appear at δ 3.74 and 3.98. Three broad singlets for 2,5-dimethyl-THF complexed in **11** were seen at δ 4.16, 4.30, and 4.46 with relative intensity of 1:2:1. We assume that, like THF, 2,5-dimethyl-THF binds so that the plane of the THF ring coincides with the plane between the Cp^* ligands. (Jordan, R. F. *Adv. Organomet. Chem.* **1991**, 32, 325. Den Haan, K. H.; De Boer, J. L.; Teuben, J. H.; Smeets, W. J. J.; Spek, A. L. *J. Organomet. Chem.* **1987**, 327, 31. Evans, W. J.; Dominguez, R.; Hanusa, T. P. *Organometallics* **1986**, 5, 263.) At -122°C , 2,5-dimethyl-THF does not rotate freely about the yttrium–oxygen bond and the two α -hydrogens of *cis*-2,5-dimethyl-THF are inequivalent. Similarly, the two α -hydrogens of complexed *trans*-2,5-dimethyl-THF are inequivalent. If *cis*- and *trans*-2,5-dimethyl-THF bind equally strongly, four equal intensity resonances are expected. The observed 1:2:1 intensity pattern is due to chemical shift degeneracy of two of the resonances. On warming, these three resonances coalesce with the free 2,5-dimethyl-THF resonances. These spectra are consistent with equal binding of the two isomers of 2,5-dimethyl-THF.

**Figure 5.** Enthalpy diagrams for monosubstituted and disubstituted alkene chelates and their nonchelated and 2,5-dimethyl-THF-bound forms.**Table 5.** Summary of ΔG_{236} , ΔH° , and ΔS° Obtained for the Equilibria between Chelating and Nonchelating Forms of **1**, **6**, **7**, and **8**

compd	ΔG_{236} (kcal mol^{-1})	ΔH° (kcal mol^{-1})	ΔS° (eu)
6-on \rightleftharpoons 6-off	-0.2	2.6	12
7-on \rightleftharpoons 7-off	2.0	4.0	8
8-on \rightleftharpoons 8-off	2.0	5.0	13
1-on \rightleftharpoons 1-off	1.2	3.2	8

mono- and disubstituted alkene binding (Figure 4). Since ΔG_{236} for the equilibrium between **6-on** and **6-off** is $-0.2 \text{ kcal mol}^{-1}$,¹⁹ ΔG_{236} for the equilibrium between chelated **7-on** and nonchelated **7-off** is $2.0 \text{ kcal mol}^{-1}$ (Figure 4 and Table 5). Equilibrium constants and free energy differences between 2,5-dimethyl-THF-bound and chelated alkyl–alkenes were calculated in a similar manner for compounds **1** and **8** (Table 4). ΔG_{236} , ΔH° , and ΔS° for alkene dissociation from the chelated complexes are presented in Table 5. ΔH° of binding for monosubstituted alkene chelates (-3.2 to $-5.0 \text{ kcal mol}^{-1}$) is an important measurement that should provide a reliable estimate of ΔH of binding of nontethered alkenes such as propene and other terminal alkenes used in commercial polymerizations.

Direct Observation of Alkene Coordination Equilibrium for a Monosubstituted Alkene Chelate. The small $1.2 \text{ kcal mol}^{-1}$ ΔG_{236} that was determined for the equilibrium between **1-on** and **1-off** suggested that **1-off** might be directly observable at higher temperatures. For example, assuming that ΔH° and ΔS° are correct, K_{eq} at 16°C should be 0.21, which corresponds to 17% **1-off**.

Temperature dependence of the alkene ^1H NMR resonances of **1** was indeed observed between -35 and 16°C . At -35°C , $\Delta\delta(\text{H}_{\text{int}}-\text{H}_{\text{trans}}) = 2.89 \text{ ppm}$, which is only slightly smaller than the 2.93 ppm observed at -50°C , but as the temperature was further increased to 16°C , $\Delta\delta(\text{H}_{\text{int}}-\text{H}_{\text{trans}})$ decreased substantially to 2.63 ppm . Equation 3,²¹ where x is the fraction chelated, was used to determine the relative amounts of **1-on** and **1-off** in solution at these temperatures (Table 6), and an van't Hoff plot gave $\Delta H^\circ = 3.3 \pm 0.1 \text{ kcal mol}^{-1}$ and $\Delta S^\circ = 9 \pm 1 \text{ eu}$. Considering the error that could have arisen from the assumptions that were made in our indirect calculations of ΔH° and ΔS° , it is fortuitous that the indirectly determined values are so similar to these directly determined values.

$$\Delta\delta(\text{H}_{\text{int}}-\text{H}_{\text{trans}}) = x(3.02) + (1 - x)(1.05) \quad (3)$$

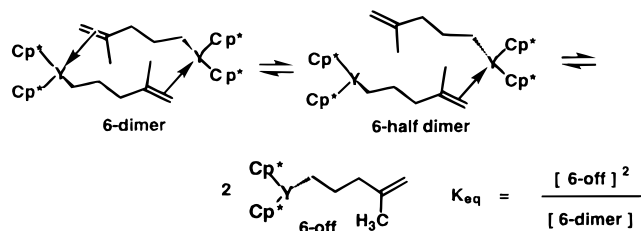
Metal–Alkyl–Alkene Complexes Are Not Dimers. Whether our d^0 ytrocene–alkyl–alkene chelate complexes are mono-

(21) The low-temperature chemical shifts of **1-on** gave $\Delta\delta(\text{H}_{\text{int}}-\text{H}_{\text{trans}}) = 3.02 \text{ ppm}$. The chemical shifts of $\text{Cp}^*_2\text{Y}(\eta^1\text{-CH}_2\text{CH}_2\text{C}(\text{CH}_3)_2\text{CH}=\text{CH}_2)$ (THF) [$\Delta\delta(\text{H}_{\text{int}}-\text{H}_{\text{trans}}) = 1.05 \text{ ppm}$] were used as estimates for **1-off**.

Table 6. $\Delta\delta(H_{\text{int}}-H_{\text{trans}})$, % **1-on**, K_{eq} , and ΔG for the Equilibrium between **1-on** and **1-off**

temp (°C)	$\Delta\delta(H_{\text{int}}-H_{\text{trans}})$ (ppm)	% 1-on	K_{eq}	ΔG (kcal mol ⁻¹)
-35	2.89	93	0.07	1.3
-23	2.84	91	0.10	1.1
-17	2.82	90	0.11	1.1
-12	2.80	89	0.13	1.1
-6	2.77	87	0.15	1.0
4	2.71	84	0.19	0.9
16	2.63	80	0.25	0.8

meric or dimeric has been a nagging question that initially could not be addressed directly. Now that we are able to measure equilibrium constants for alkene coordination, we can resolve the question. If the d⁰ yttrocene-alkyl-alkene were a dimer, the equilibrium between coordinated alkene and free alkene would be concentration dependent; but if it is a monomer, then the equilibrium would be concentration independent (Scheme 6). We have found that the equilibrium between **6-on** and **6-off** is concentration independent.



When 0.0085 and 0.023 M solutions of **6** were examined by ¹H NMR spectroscopy between -51 and -90 °C, very nearly identical chemical shift differences between the terminal vinyl protons were observed over the entire temperature range. Therefore, the percentages of **6-on** and **6-off** were nearly identical for the two samples. For example, at -51 °C, both the 0.0085 M and the 0.023 M solutions of **6** had $\Delta\delta = 0.34$ ppm, corresponding to 50% chelate **6-on**.²² Clearly our data is inconsistent with a dimer–monomer equilibrium.

Another suggested alternative is a dimeric system which dissociates one alkene to give a half-coordinated dimer. This alternative could explain the concentration independence of the coordination equilibria only if the half dimer failed to dissociate to a significant degree. It is more likely that the second dissociation would be more favorable than the first dissociation from the chelated dimer. If the half dimer were the only species with a free alkene, then no more than 50% alkene dissociation would have been observed.

Discussion

The direct NMR observation of chelated yttrium-alkyl-alkene complexes has established the viability of d⁰ metal-alkyl-alkene intermediates in Ziegler–Natta polymerizations. The shifts of the NMR resonances of the internal alkene carbon and its attached hydrogen to higher frequency are consistent with polarization of the C=C double bond produced by coordination to the electron deficient yttrium center. This polarization in part explains the rapid addition of negatively polarized alkyl metal carbon centers to the complexed alkene

(22) Equilibrium constants were calculated assuming that the system is both monomeric and dimeric. Assuming a monomeric system, K_{eq} was determined to be 1.0 at -51 °C for both the 0.0085 and 0.023 M solutions of **6**. Assuming a dimeric system, the computed K_{eq} for the 0.0085 M solution of **6** was 7.1×10^{-5} M and the computed K_{eq} for the 0.023 M solution of **6** was 5.4×10^{-4} M.

and helps to account for the rapid rates of Ziegler–Natta polymerizations.

Binding Energies of Alkenes to d⁰ Yttrium Alkyls. Our ability to directly observe chelated metal-alkyl-alkene complexes has now allowed us to measure the equilibrium constants for alkene binding and the associated binding energies. A major breakthrough was the observation of temperature dependent chemical shifts for the disubstituted alkene chelate complex **6**. This provided direct evidence for an equilibrium between chelated **6-on** and nonchelated **6-off** and allowed us to measure the equilibrium constants for alkene coordination over a wide temperature range.

We were particularly interested in determining ΔH° of binding because these values should be similar to those of nonchelated alkenes used in polymerization. For the disubstituted alkene chelate **6**, the equilibrium constant for alkene complexation (**6-on**:**6-off**) was 50% **6-on** and 50% **6-off** at -51 °C, and 32% **6-on** and 68% **6-off** at -22 °C ($\Delta G_{236} = -0.2$ kcal mol⁻¹). ΔH° for the disubstituted alkene binding was 2.6 ± 0.2 kcal mol⁻¹. We were even more interested in the binding energies of monosubstituted alkene chelates because these compounds provide better models for propene and other terminal alkenes important in polymerizations. However, because these monosubstituted chelates showed little evidence for alkene dissociation at low temperature, we used an indirect method to measure their binding energies. We found that 2,5-dimethyl-THF coordinated to monosubstituted chelate complexes **1**, **7**, and **8** less tightly than to disubstituted chelate **6**. The difference in the free energy of 2,5-dimethyl-THF binding gives the free energy difference between mono- and disubstituted alkene binding. For monosubstituted alkene complexes **7** and **8**, $\Delta G(236 \text{ K})$ of alkene binding was 2.2 kcal mol⁻¹ greater than that for disubstituted alkene chelate **6**. Because of larger errors in measuring ΔH and ΔS than in measuring ΔG and because ΔS should be the same for displacement of all the chelates by 2,5-dimethyl-THF, we believe the difference in ΔH and ΔG should be the same for all the chelates. Therefore, a reasonable estimate for ΔH of binding of monosubstituted alkene chelates **7** and **8** is 4.8 ± 0.5 kcal mol⁻¹.

The greater binding energy of mono- than disubstituted alkene chelates is consistent with the observation that monosubstituted alkenes are much more easily polymerized than disubstituted alkenes in Ziegler–Natta copolymerizations with ethylene.¹ Brookhart found that ethylene binds 0.9 kcal mol⁻¹ (ΔG) more strongly than propene to $(\text{ArN}=\text{CHCH}=\text{NAr})\text{PdCH}_3^+$ at -85 °C.²³ Similarly, propene binds 2.5 kcal mol⁻¹ more tightly than the disubstituted alkene isobutene to $\text{Rh}(\text{acac})(\text{C}_2\text{H}_4)$ at 25 °C.²⁴

The ΔH of binding of monosubstituted alkenes to the d⁰ yttrium centers of **7** and **8** (4.8 ± 0.5 kcal mol⁻¹) is much smaller than the binding energy of alkenes to late transition metals. The binding energy of cyclooctene to $\text{CpMn}(\text{CO})_2$ ²⁵ is 24.5 kcal mol⁻¹, and that of 1-hexene in $\text{Cr}(\text{CO})_5(\text{CH}_2=\text{CHCH}_2-\text{CH}_2\text{CH}_2\text{CH}_3)$ ²⁶ is 12.2 kcal mol⁻¹. Ethylene displaces the ketone carbonyl from $(\text{phen})\text{Pd}(\eta^1, \eta^1-\text{CH}_2\text{CH}_2\text{C}(\text{CH}_3)=\text{O})$ and binds 7.8 kcal mol⁻¹ more tightly.²⁷ Ziegler has calculated a 19.4 kcal mol⁻¹ ethylene binding energy for $(\text{HN}=\text{CH}-\text{CH}=\text{NH})\text{Ni}-(\text{CH}_2\text{CH}_2\text{CH}_3)(\text{H}_2\text{C}=\text{CH}_2)^+$.²⁸

(23) Mecking, S.; Johnson, L. K.; Wang, L.; Brookhart, M. *J. Am. Chem. Soc.* **1998**, *120*, 888.

(24) Cramer, R. *J. Am. Chem. Soc.* **1967**, *89*, 4621.

(25) Klassen, J. K.; Selke, M.; Sorensen, A. A.; Yang, G. K. *J. Am. Chem. Soc.* **1990**, *112*, 1267.

(26) Klassen, J. K.; Yang, G. K. *Organometallics* **1990**, *9*, 874.

(27) Rix, F. C.; Brookhart, M. *J. Am. Chem. Soc.* **1995**, *117*, 1137.

(28) Deng, L.; Margl, P.; Ziegler, T. *J. Am. Chem. Soc.* **1997**, *119*, 1094.

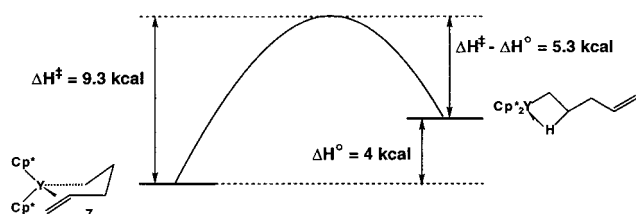


Figure 6. Enthalpies of alkene dissociation and alkene binding for $\text{Cp}^*_2\text{Y}[\eta^1, \eta^2\text{-CH}_2\text{CH}_2\text{CH}_2\text{CH}=\text{CH}_2]$ (**7**).

A significantly smaller ΔH° of alkene binding of $4.0 \text{ kcal mol}^{-1}$ was estimated for the monosubstituted chelate complex **1**, which has a *gem*-dimethyl group on the tether, based on smaller equilibrium constants for complexation of 2,5-dimethyl-THF. This weaker alkene binding was confirmed by observation of temperature dependent vinyl chemical shifts for **1** which gave ΔH° of 3.1, similar to the value determined indirectly from 2,5-dimethyl-THF equilibria. The smaller binding energy of the dimethyl-substituted chelate is explained by steric destabilization of the chelate ring. Molecular mechanics calculations (UFF2 implemented in Cerius²⁹) for the nonmethylated chelate **7** show a preferred chair conformation for the chelate ring. With two methyl groups on the chelate tether, the chair conformation is destabilized by an axial methyl– Cp^* interaction, and the twist-boat conformation is preferred. Thus our original design of a dimethyl substituted chelate to promote ring formation (Thorpe–Ingold effect)³⁰ was actually counterproductive and the *gem*-dimethyl group on the tether actually disfavors chelate formation.^{8a}

The fact that the binding energy for the monosubstituted alkenes is so small explains why d^0 metal–alkyl–alkene complexes have been observed only when the alkene is tethered to another ligand. With our estimate of $\Delta H^\circ = 4\text{--}5 \text{ kcal mol}^{-1}$ for monosubstituted alkene binding, we can address the question of whether it will be possible to observe alkene complexation for simple alkenes like propene. If we assume a typical range of $\Delta S^\circ = -25$ to -35 eu for formation of a bimolecular complex, we can calculate that at $-145 \text{ }^\circ\text{C}$, the lowest temperature we can access by NMR, ΔG will be in the range -1.4 to $1.0 \text{ kcal mol}^{-1}$. For the most favorable case, K_{eq} will be 300 M^{-1} and more than 80% of the yttrium alkyl will have propene complexed at 0.02 M propene. In the least favorable case, K_{eq} will be $1.6 \times 10^{-2} \text{ M}^{-1}$ and only 0.03% of the yttrium alkyl will have propene complexed at 0.02 M propene. Clearly, a concerted effort to observe a nonchelated metal–alkyl–alkene complex is a worthwhile and challenging endeavor that we are currently pursuing.

Kinetics of Alkene Decomplexation. The enthalpic barrier (ΔH^\ddagger) for alkene dissociation and recomplexation from the opposite enantioface of the double bond is substantially larger than the alkene binding enthalpy (ΔH°) (Figure 6). The enthalpy of alkene dissociation and recomplexation to the opposite face for $\text{Cp}^*_2\text{Y}[\eta^1, \eta^2\text{-CH}_2\text{CH}_2\text{CH}_2\text{CH}=\text{CH}_2]$ (**7**) ($\Delta H^\ddagger = 9.3 \pm 0.3 \text{ kcal mol}^{-1}$) is $5.3 \text{ kcal mol}^{-1}$ greater than the alkene binding enthalpy ($\Delta H^\circ = 4 \pm 1 \text{ kcal mol}^{-1}$). The significantly greater ΔH^\ddagger compared with ΔH° can be attributed either to stabilization of dissociated yttrium alkyl **7-off** or to destabilization of the transition state leading to alkene dissociation.

7-off is expected to be stabilized by a β -agostic interaction while neither **7-on** nor the transition state leading to **7-off** is

expected to have such stabilization. A β -agostic interaction is sterically impossible for **7-on**, and there is no evidence for an α -agostic interaction for **7-on**. Evidence for a β -agostic interaction in the saturated alkyl yttrium complex $\text{Cp}^*_2\text{YCH}_2\text{CH}_2\text{-CHCH}_3\text{CH}_2\text{CH}_3$ related to **7-off** was obtained from the decreased magnitude of the $^1J_{\text{CH}}$ coupling of the β - CH_2 group ($^1J_{\text{CH}} = 109 \text{ Hz}$) compared to the chelate complexes **1-on**, **7-on**, and **8-on** ($^1J_{\text{CH}} = 125 \text{ Hz}$). Therefore, a large fraction of the 5 kcal mol^{-1} stabilization of **7-off** relative to the transition state can be attributed to a β -agostic interaction formed after alkene dissociation.

An alternative explanation for the 5 kcal mol^{-1} difference between ΔH^\ddagger and ΔH° involves the development of steric strain in the transition state for alkene dissociation. For dissociation of a simple nonchelated ligand, ΔH^\ddagger and ΔH° should be very similar. However, for a chelate, ΔH^\ddagger can be substantially greater than ΔH° because of the added strain in the tether during alkene movement to and from the crowded metal center.

For the *gem*-dimethyl chelate complex $\text{Cp}^*_2\text{Y}[\eta^1, \eta^2\text{-CH}_2\text{-CH}_2\text{C}(\text{Me})_2\text{CH}=\text{CH}_2]$ (**1**), a larger difference of $7.0 \text{ kcal mol}^{-1}$ is seen between the enthalpy of alkene dissociation ($\Delta H^\ddagger = 10.2 \pm 0.4 \text{ kcal mol}^{-1}$) and the alkene binding enthalpy ($\Delta H^\circ = 3.2 \pm 0.7 \text{ kcal mol}^{-1}$). The *gem*-dimethyl group of **1** may be responsible for added steric hindrance to alkene movement from and to the crowded yttrium center. The disubstituted alkene chelate $\text{Cp}^*_2\text{Y}[\eta^1, \eta^2\text{-CH}_2\text{CH}_2\text{CH}_2\text{C}(\text{CH}_3)_2\text{CH}=\text{CH}_2]$ (**6**) has an even larger difference of $8.3 \text{ kcal mol}^{-1}$ between the enthalpy of alkene dissociation ($\Delta H^\ddagger = 10.9 \pm 0.3 \text{ kcal mol}^{-1}$) and the alkene binding enthalpy ($\Delta H^\circ = 2.6 \pm 0.1 \text{ kcal mol}^{-1}$). Passage of the more sterically demanding disubstituted alkene of chelate **6** past the Cp^* ligands might pose a more formidable steric obstacle to the dissociation and recomplexation of the alkene.

A corollary to ΔH^\ddagger being greater than ΔH° for chelates is that nonchelated alkenes such as propene should exchange much more rapidly than chelates. Since the barriers for alkene dissociation from yttrium chelates are already quite low, exchange of propene should be exceedingly rapid; ΔH^\ddagger barriers similar to ΔH° of $3\text{--}5 \text{ kcal mol}^{-1}$ can be anticipated.

The binding energy of an alkene to a cationic group(IV) metal center should be stronger than binding of an alkene to a neutral group(III) metal center because of the charge-induced dipole interaction. If part of the barrier to alkene dissociation is due to the alkene binding energy, then a higher barrier would be expected for a zirconium(IV) alkene complex. This is consistent with experimental data from our group and Jordan's. The two diastereomers of $\text{Cp}^*_2\text{Zr}[\eta^1, \eta^2\text{-CH}_2\text{CH}\{\text{CH}_2\text{B}(\text{C}_6\text{F}_5)_3\}\text{CH}_2\text{CH}=\text{CH}_2]$ (**5**) are interconverted by alkene dissociation and recoordination from the opposite face ($\Delta G^\ddagger(-42 \text{ }^\circ\text{C}) = 10.5 \text{ kcal mol}^{-1}$).⁷ A similar barrier for alkene dissociation and recomplexation was reported for the zirconium(IV) oxypent-4-enyl chelate complex **2** ($\Delta G^\ddagger = 10.7 \pm 0.1 \text{ kcal mol}^{-1}$).⁴ These barriers are $3\text{--}4 \text{ kcal mol}^{-1}$ higher than the analogous free energies of activation measured for chelate complexes **1** and **7**.

Kinetics of Inversion at Yttrium. The free energy of activation for interconversion of the diastereotopic Cp^* ligands of chelate **8** by alkene dissociation combined with inversion at yttrium ($\Delta G^\ddagger(-72 \text{ }^\circ\text{C}) = 9.6 \pm 0.3 \text{ kcal mol}^{-1}$) is about 2 kcal mol^{-1} greater than the barrier for alkene dissociation without inversion at yttrium that interconverts Cp^* ligands on complexes **1**, **6**, and **7** and is four times greater than the binding energy of the pendant alkene ($\Delta G(-72 \text{ }^\circ\text{C}) = 2.4 \text{ kcal mol}^{-1}$) (Scheme 6). Starting from the alkene dissociated intermediate **8-off**, a barrier to net inversion at the metal center of $7.2 \text{ kcal mol}^{-1}$ is incurred. This barrier may arise from three sources: (1) an

(29) (a) Rappé, A. K.; Casewit, C. J.; Colwell, K. S.; Goddard, W. A.; Skiff, W. M. *J. Am. Chem. Soc.* **1992**, *114*, 10024. (b) Rappé, A. K.; Colwell, K. S.; Casewit, C. J. *Inorg. Chem.* **1993**, *32*, 3438.

(30) For a brief description of the Thorpe–Ingold effect, see: Eliel, E. L. *Stereochemistry of Carbon Compounds*; McGraw-Hill: New York, 1962; pp 196–198. Eliel, E. L.; Allinger, N. L.; Angyal, S. J.; Morrison, G. A. *Conformational Analysis*; Interscience: New York, 1965; pp 191–192.

Scheme 6

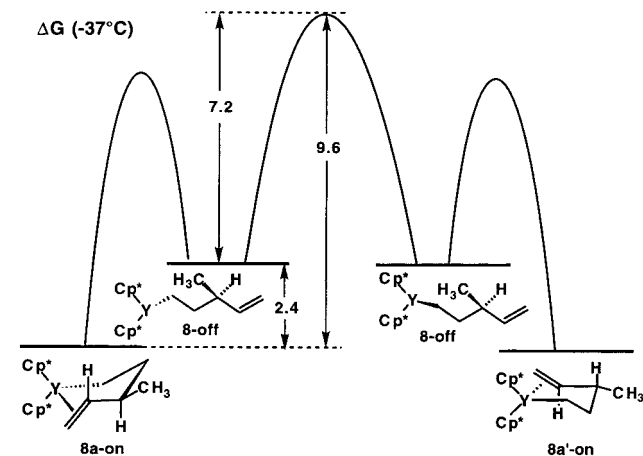
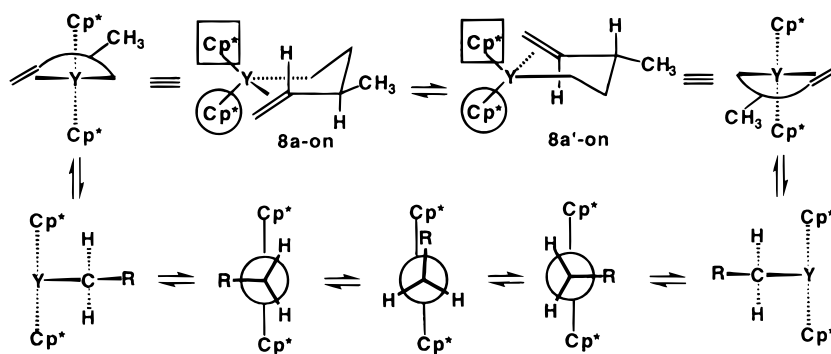


Figure 7. Free energy diagram for alkene binding and the barrier to alkene dissociation combined with inversion at yttrium for $\text{Cp}^*_2\text{YCH}_2\text{-CH}_2\text{CH}(\text{CH}_3)\text{CH}=\text{CH}_2$ (**8**).

intrinsic barrier to inversion of a pyramidal yttrium center,³¹ (2) the loss of an agostic interaction³² (if any), which has been proposed to stabilize d^0 metal–alkyl–alkene complexes, and (3) a 180° rotation about the $\text{Y}-\text{CH}_2$ bond, during which the alkyl chain must pass one of the Cp^* ligands (Scheme 6).

For Royo's zirconocene-alkene chelate **3**, diastereotopic hydrogens are equilibrated by alkene dissociation followed by inversion at zirconium ($\Delta G^\ddagger(-72^\circ\text{C}) = 11.9 \text{ kcal mol}^{-1}$, $\Delta H^\ddagger = 12.9 \pm 0.5 \text{ kcal mol}^{-1}$, and $\Delta S^\ddagger = 5.0 \pm 2.3 \text{ eu}$).³³ Both ΔG^\ddagger and ΔH^\ddagger are about 2 kcal mol^{-1} greater for **3** than for yttrium complex **8**, consistent with a stronger metal–alkene bond to cationic zirconium.^{34,35}

Ziegler–Natta polymerization of propene by d^0 metallocene catalysts can proceed with high stereospecificity.^{1c} For C_s - and

C_1 -symmetric catalysts, the stereochemistry of polypropylene depends on the rate of inversion at the pyramidal metal center relative to chain extension. In the proposed model for stereocontrol,³⁶ the growing polymer chain is positioned to avoid steric interactions with the metallocene ligands; this geometry is reinforced by an α -agostic interaction. Propene coordinates to minimize interaction between its methyl group and the polymer chain. On the basis of this model, the production of syndiotactic propylene by Ewen's C_s -symmetric catalyst **15** relies on slow inversion at the metal compared to alkene coordination and insertion (Scheme 7).^{36a,37} Accordingly, C_s -symmetric zirconocene catalysts produce more highly syndiotactic polypropylene at higher propene concentrations, when the rate of alkene coordination and insertion is accelerated relative to inversion at the metal center.^{36a,38} Inversion at the metal center of C_1 -symmetric catalyst **16** was proposed by Marks to be rapid relative to alkene coordination and insertion so that chain propagation occurs from only one sterically favored invertomer and isotactic polypropylene is formed (Scheme 8).^{36a,38,39} This conclusion is supported by the observation that polypropylene isotacticity decreases with increasing propene concentration for related C_1 -symmetric zirconocene catalysts.^{36a,37e,38} C_2 -Symmetric metallocenes^{37c,e,40} such as **17** produce highly isotactic polypropylene regardless of the rate of inversion at the metal because the same enantioface of propene coordinates to both of the C_2 -related sites.

Alkene Dissociation from d^0 Yttrium–Alkyl–Alkene Complexes Is Much Faster than Insertion. To understand

(35) For the related d^2 complex $[\text{Me}_2\text{Si}(\text{C}_5\text{Me}_4)_2]\text{Ta}(\eta^2\text{-C}_2\text{H}_4)\text{H}$, interchange of the environments of the diastereotopic methyl groups on the Me_2Si *ansa* bridge and C_5Me_4 rings has been observed. This process requires alkene insertion into the $\text{Ta}-\text{H}$ bond to form $[\text{Me}_2\text{Si}(\text{C}_5\text{Me}_4)_2]\text{Ta}(\text{CH}_2\text{CH}_3)$, inversion at tantalum, and β -hydride elimination to the ethylene hydride complex. The activation barrier is $\Delta G^\ddagger(25^\circ\text{C}) = 17.0 \text{ kcal mol}^{-1}$. Shin, J. H.; Parkin, G. *Chem. Commun.* **1999**, 887.

(36) (a) Veghini, D.; Henling, L. M.; Burkhardt, T. J.; Bercaw, J. E. *J. Am. Chem. Soc.* **1999**, *121*, 564. (b) Guerra, G.; Cavallo, L.; Moscardi, G.; Vacatello, M.; Corradini, P. *J. Am. Chem. Soc.* **1994**, *116*, 2988. (c) Corradini, P.; Guerra, G.; Vacatello, M.; Villani, V. *Gazz. Chim. Ital.* **1988**, *118*, 173.

(37) (a) Mitchell, J. P.; Hajela, S.; Brookhart, S. K.; Hardcastle, K. I.; Henling, L. M.; Bercaw, J. E. *J. Am. Chem. Soc.* **1996**, *118*, 1045. (b) Ewen, J. A.; Jones, R. L.; Razavi, A.; Ferrara, J. D. *J. Am. Chem. Soc.* **1988**, *110*, 6255. (c) Ewen, J. A.; Elder, M. J.; Jones, R. L.; Haspelslagh, L.; Atwood, J. L. Bott, S. G.; Robinson, K. *Makromol. Chem., Macromol. Symp.* **1991**, *48/49*, 253. (d) Ewen, J. A.; Elder, M. J. *Makromol. Chem., Macromol. Symp.* **1993**, *66*, 179. (e) Ewen, J. A. *Makromol. Chem., Macromol. Symp.* **1995**, *89*, 181.

(38) Herzog, T. A.; Zubris, D. L.; Bercaw, J. E. *J. Am. Chem. Soc.* **1996**, *118*, 11988.

(39) (a) Giardello, M. A.; Eisen, M. S.; Stern, C. L.; Marks, T. J. *J. Am. Chem. Soc.* **1995**, *117*, 12114. (b) Miyake, S.; Okumura, Y.; Inazawa, S. *Macromolecules* **1995**, *28*, 3074.

(40) (a) Wild, F. R. W. P.; Wasiucioneck, M.; Huttner, G.; Brintzinger, H. H. *J. Organomet. Chem.* **1985**, *288*, 63. (b) Resconi, L.; Piemontesi, F.; Camurati, I.; Sudmeijer, O.; Nifant'ev, I. E.; Ivchenko, P. V.; Kuz'mina, L. G. *J. Am. Chem. Soc.* **1998**, *120*, 2308.

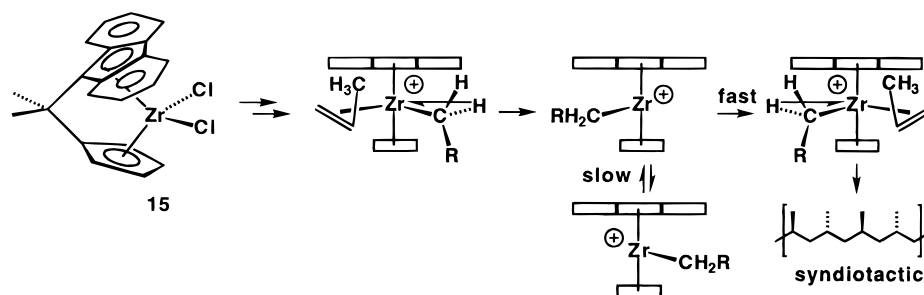
(31) DFT and ab initio calculations predict a planar structure for methyl complexes of d^0 -metallocenes such as Cp_2ScCH_3 . For ethyl and propyl-metallocene complexes, the d^0 metal center is predicted to adopt a pyramidal geometry in order to accommodate an energetically favorable β -CH agostic interaction. (a) Ziegler, T.; Folga, E.; Berces, A. *J. Am. Chem. Soc.* **1993**, *115*, 636. (b) Woo, T. K.; Fan, L.; Ziegler, T. *Organometallics* **1994**, *13*, 2252. (c) Yoshida, T.; Koga, N.; Morokuma, K. *Organometallics* **1995**, *14*, 746. (d) Weiss, H.; Ehrig, M.; Ahlrichs, R. *J. Am. Chem. Soc.* **1994**, *116*, 4919. (e) Kawamura-Kuribayashi, H.; Koga, N.; Morokuma, K. *J. Am. Chem. Soc.* **1992**, *114*, 8687.

(32) (a) Brookhart, M.; Green, M. L. H. *J. Organomet. Chem.* **1983**, *250*, 395. (b) Brookhart, M.; Green, M. L. H.; Wong, L.-L. *Prog. Inorg. Chem.* **1988**, *36*, 1. (c) Grubbs, R. H.; Coates, G. W. *Acc. Chem. Res.* **1996**, *29*, 85.

(33) Galakhov, M. V.; Heinz, G.; Royo, P. *Chem. Commun.* **1998**, 17.

(34) Marks has reported the equilibration of the methyl groups of $(1,2\text{-Me}_2\text{C}_5\text{H}_3)_2\text{ZrCH}_3^+\text{CH}_3\text{B}(\text{C}_6\text{F}_5)_3^-$ by ion pair dissociation and inversion at zirconium. The enthalpic barrier for this process is 12 kcal mol^{-1} in chlorobenzene- d_5 and 24 kcal mol^{-1} in toluene- d_8 , in which ion pair separation is not solvent assisted. Deck, P. A.; Marks, T. J. *J. Am. Chem. Soc.* **1995**, *117*, 6128.

Scheme 7



Scheme 8

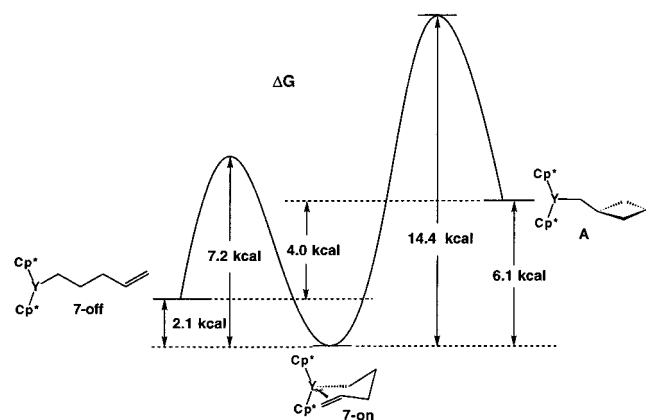
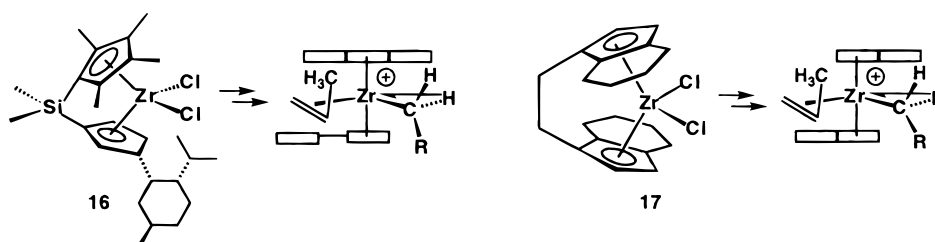


Figure 8. Free energy diagram for chelate **7-on**, η^1 -alkyl complex **7-off**, and cyclobutylmethyl intermediate **A**.

ligand control of stereochemistry in metallocene catalyzed polymerizations, it is crucial to know whether stereochemistry is controlled by irreversible alkene approach or by the stereochemistry of the alkene insertion step. Earlier, we measured the rate of intramolecular alkene insertion into an yttrium chelate by an isotopic labeling experiment. Exchange of CD_2 into the γ -position of $\text{Cp}^*_2\text{Y}[\eta^1, \eta^2\text{-CD}_2\text{CH}_2\text{CH}_2\text{CH}=\text{CD}_2]$ (**7-d₄**) occurs by reversible alkene insertion to give an unstable cyclobutylmethyl intermediate **A** (Figure 8). At -78°C , the half-life for exchange was about 40 min, corresponding to $\Delta G^\ddagger = 14.4 \pm 0.1 \text{ kcal mol}^{-1}$. We have now measured $\Delta G^\ddagger(-78^\circ\text{C}) = 7.2 \text{ kcal mol}^{-1}$ for alkene dissociation from **7** by dynamic NMR spectroscopy. Thus, the barrier for alkene dissociation is $7.2 \text{ kcal mol}^{-1}$ lower than for insertion to make the cyclobutylmethyl intermediate, and alkene dissociation is 10^8 faster than insertion!

The much more rapid alkene dissociation relative to alkene insertion seen for chelate complex **7** should also be seen for nonchelated systems. However, the relative rates may be substantially different. The insertion of alkene into chelate **7** should be unusually slow due to formation of the highly strained cyclobutylmethyl intermediate. Alkene decomplexation might also be slower for chelate complex **7** due to added strain in the chelate backbone at the transition state for alkene dissociation (ΔH^\ddagger is $5.3 \text{ kcal mol}^{-1} > \Delta H^\circ$). It will be interesting to see

how the rates of alkene dissociation and insertion compare for nonchelated systems.

While our results clearly demonstrate that alkene dissociation from yttrium is much faster than insertion, extrapolation of these results to cationic titanium and zirconium catalysts is problematic. Alkene dissociation from more electrophilic zirconium cations is expected to be much slower than from neutral yttrium centers, and our recent study shows that alkene dissociation from cationic zirconium chelate $\text{Cp}^*_2\text{Zr}[\eta^1, \eta^2\text{-CH}_2\text{CH}\{\text{CH}_2\text{B}(\text{C}_6\text{F}_5)_3\}\text{-CH}_2\text{CH}=\text{CH}_2]$ (**5**)⁷ has a barrier 2 kcal higher than those measured for yttrium chelate complexes **1**, **6**, and **7**. In contrast, the rate of alkene insertion is expected to be much faster for a cationic zirconium complex than for a neutral yttrium complex. It will be interesting to obtain an experimental comparison of alkene dissociation and insertion rates for titanium and zirconium centers.

Experimental Section⁴¹

$\text{Cp}^*_2\text{Y}[\eta^1, \eta^2\text{-CH}_2\text{CH}_2\text{CH}_2\text{C}(\text{CH}_3)=\text{CH}_2]$ (**6**) in Methylcyclohexane- d_{14} /Pentane- d_{12} . 2-Methyl-1,4-pentadiene (0.024 mmol) was condensed into an NMR tube containing $(\text{Cp}^*_2\text{YH})_2$ (0.009 mmol, prepared in situ) and $\text{CH}_2(\text{SiMe}_3)_2$ (which was used as an internal standard) in a mixture of approximately 1:1 methylcyclohexane- d_{14} /pentane- d_{12} (0.55 mL). The tube was sealed and shaken intermittently at -78°C for about 2 min. ^1H NMR spectroscopy showed a 70% yield of **6** along with 2-methyl-1-pentene (10%). ^1H NMR (500 MHz, $\text{C}_6\text{D}_{11}\text{CD}_3/\text{C}_5\text{D}_{12}$, -142°C): δ -0.70 (br s, $\omega_{1/2} = 56 \text{ Hz}$, YCHH), -0.18 (br s, partially obscured by $\text{CH}_2(\text{Si}(\text{CH}_3)_3)_2$ resonances, YCHH), 1.28 (m, YCH_2CH_2), 1.62 (s, CH_3), 1.88, 1.93 (two br s; $\omega_{1/2} = 15 \text{ Hz}$, 11 Hz; diastereotopic Cp^* resonances), 3.73 (br s, $\omega_{1/2} = 27 \text{ Hz}$, =CHH), 4.37 (br s, $\omega_{1/2} = 30 \text{ Hz}$, =CHH). Resonances for 2-methyl-1,4-pentadiene: δ 0.88 (t, $\text{CH}_2\text{CH}_2\text{CH}_3$), 1.46 (m, $\text{CH}_2\text{CH}_2\text{CH}_3$), 1.62 (s, $\text{CH}_2=\text{C}(\text{CH}_3)$), 4.63, 4.66 (two s, 2H, $\text{CH}_2=\text{C}(\text{CH}_3)$), $\text{CH}_2\text{CH}_2\text{CH}_3$ obscured by Cp^* resonance.¹⁵

The temperature dependence of the chemical shifts of the vinyl hydrogen resonances and $\alpha\text{-CH}_2$ resonances were measured between -29 and -142°C . (See Supporting Information: Table 1; Figures 1 and 11.) Above -40°C , slow decomposition of **6** occurs and numerous additional peaks grow between δ -0.5 and 2.0 ; resonances in this region were difficult to assign, but vinyl resonances were readily assigned. At -15°C , **6** decomposes within 5 min. ^1H NMR (500 MHz, $\text{C}_6\text{D}_{11}\text{-CD}_3/\text{C}_5\text{D}_{12}$, -29°C): δ 1.91 (s, Cp^*), 4.22 (br s, $\omega_{1/2} = 35 \text{ Hz}$, =CHH), 4.46 (br s, $\omega_{1/2} = 35 \text{ Hz}$, =CHH).

(41) See Supporting Information for General Procedures.

Cp*₂Y[η¹-CH₂CH₂CH₂C(CH₃)=CH₂](2,5-dimethyl-THF) (10). 2,5-Dimethyl-THF (0.027 mmol) was condensed into an NMR tube containing Cp*₂Y[η¹,η²-CH₂CH₂CH₂C(CH₃)=CH₂] (**6**) (0.017 mmol, prepared in situ) and CH₂(SiMe₃)₂ (which was used as an internal standard) in a solution of approximately 1:1 methylcyclohexane-*d*₁₄/pentane-*d*₁₂ (0.54 mL). The tube was sealed and shaken intermittently at -78 °C for about 2 min. The yellow solution turned colorless. ¹H NMR spectroscopy showed formation of **10** in 90% yield. At -65 °C, only **10** and no **6** are present. ¹H NMR (500 MHz, C₆D₁₁CD₃/C₅D₁₂, -65 °C): δ -0.48 (br m, ω_{1/2} = 25 Hz, YCH₂); 1.31 (m, YCH₂CH₂); 1.47 (br m, ω_{1/2} = 21 Hz, β-THF); 1.68 (s, CH₃); 1.92 (s, Cp*); 4.05, 4.23 (two br s; ω_{1/2} = 24, 24 Hz; α-CH of *cis*- and *trans*-2,5-dimethyl-THF); 4.53 (br s, ω_{1/2} = 6 Hz, =CHH); 4.57 (br s, ω_{1/2} = 8 Hz, =CHH); resonance for Cp*₂YCH₂CH₂CH₂ obscured by Cp* resonance.

The temperature dependence of the chemical shifts of the vinyl hydrogen resonances were measured at -33, -36, -42, -45, -51, -55, and -65 °C. (See Supporting Information: Tables 2 and 3; Figures 2 and 13.) At -33 °C, the solution contains 89% **10** and 11% chelate **6**. ¹H NMR (500 MHz, C₆D₁₁CD₃/C₅D₁₂, -33 °C): δ -0.31 (br m, ω_{1/2} = 21 Hz, YCH₂); 1.31 (m, YCH₂CH₂); 1.45 (br m, ω_{1/2} = 15 Hz, β-2,5-dimethyl-THF); 1.65 (s, CH₃); 1.92 (s, Cp*); 3.97, 4.18 (two br m; ω_{1/2} = 20, 17 Hz; α-CH of 2,5-dimethyl-THF); 4.44 (d, J_{gem} = 3 Hz, =CHH), 4.53 (d, J_{gem} = 3 Hz, =CHH), resonance for Cp*₂YCH₂CH₂CH₂ obscured by Cp* resonance.

Cp*₂Y[η¹-CH₂CH₂CH₂CH=CH₂](2,5-dimethyl-THF) (11). 2,5-Dimethyl-THF (0.062 mmol) was condensed into an NMR tube containing Cp*₂Y[η¹,η²-CH₂CH₂CH₂CH=CH₂] (**7**) (0.017 mmol, prepared in situ) and CH₂(SiMe₃)₂ (which was used as an internal standard) in a solution of approximately 1:1 methylcyclohexane-*d*₁₄/pentane-*d*₁₂ (0.45 mL). The tube was sealed and shaken intermittently at -78 °C for about 2 min. The solution changed from yellow to colorless. ¹H NMR spectroscopy showed formation of **11** in 82% yield. At -122 °C, only **11** and no **7** are present. ¹H NMR (500 MHz, C₆D₁₁CD₃/C₅D₁₂, -122 °C): δ -0.62 (br s, ω_{1/2} = 61 Hz, YCHH); -0.34 (br s, partially obscured by CH₂(SiMe₃)₂, YCHH); 1.32 (m, YCH₂CH₂); 1.37 (br m, ω_{1/2} = 26 Hz, β-CH₂ of *cis*- and *trans*-2,5-dimethyl-THF); 1.91 (br s, ω_{1/2} = 46 Hz, Cp*); 3.76, 3.99 (two br s; ω_{1/2} = 19, 19 Hz; α-CH of uncoordinated *cis*- and *trans*-2,5-dimethyl-THF); 4.16, 4.30, 4.46 (three br s, 1:2:1 ratio; ω_{1/2} = 30, 34, 38 Hz; α-CH coordinated *cis*- and *trans*-2,5-dimethyl-THF); 4.77 (br s, ω_{1/2} = 22 Hz, =CHH); 4.86 (d, J_{trans} = 16 Hz, =CHH); 5.78 (br s, partially obscured by resonance of excess diene, CH=CH₂); resonance for YCH₂CH₂CH₂ obscured by Cp* resonance. At -69 °C, the solution contains 85% **11** and 15% chelate **7**. ¹H NMR (500 MHz, C₆D₁₁CD₃/C₅D₁₂, -69 °C): δ -0.44 (br s, ω_{1/2} = 26 Hz, YCH₂); 1.30 (m, YCH₂CH₂); 1.41 (br m,

ω_{1/2} = 17 Hz, β-THF); 1.92 (s, Cp*); 3.87, 4.09 (two br s; ω_{1/2} = 23, 23 Hz; α-2,5-dimethyl-THF); 4.66 (br s, ω_{1/2} = 133 Hz, =CHH); 5.89 (br s, ω_{1/2} = 120 Hz, CH=CH₂); resonances for YCH₂CH₂CH₂ and =CHH obscured by Cp* resonance and excess diene resonance, respectively.

Variable-Temperature ¹H NMR Spectra of Cp*₂Y[η¹-CH₂CH₂CH=CH₂](2,5-dimethyl-THF) (11). The temperature dependence of the chemical shifts of the alkene resonances of a solution of **11** (0.028 M) and excess 2,5-dimethyl-THF (0.116 M) in approximately 1:1 methylcyclohexane-*d*₁₄/pentane-*d*₁₂ was measured at -33, -37, -42, -49, -51, -56, -60, -67, -71, -76, and -85 °C. (See Supporting Information: Tables 4 and 5; Figures 3, 4, and 14.) Two spectra are reported: at -37 °C, for a mixture of 26% **11** and 74% chelate **7**, and at -85 °C, for a mixture of 98% **11** and 2% chelate **7**. ¹H NMR (500 MHz, C₆D₁₁CD₃/C₅D₁₂, -37 °C): δ -0.34 (td; ³J = 7 Hz, J_{YH} = 4 Hz, YCH₂); 1.30 (m, YCH₂CH₂); 1.40 (m, β-CH₂ of *cis*- and *trans*-2,5-dimethyl-THF); 1.93 (s, Cp*); 3.83, 4.06 (two q; ³J = 5, 5 Hz; α-CH of *cis*- and *trans*-2,5-dimethyl-THF); 4.12 (dd; J_{cis} = 10 Hz, J_{gem} = 3 Hz, =CHH); 5.22 (dd; J_{trans} = 17 Hz, J_{gem} = 3 Hz; =CHH); 6.44 (m, CH=CH₂), resonance for YCH₂CH₂CH₂ obscured by Cp* resonance. At -85 °C: δ -0.45 (br s, ω_{1/2} = 48 Hz, YCH₂); 1.29 (m, YCH₂CH₂); 1.42 (br s, ω_{1/2} = 26 Hz, β-THF); 1.92 (s, Cp*); 3.85, 4.08 (two br s; ω_{1/2} = 62, 53 Hz; α-CH of *cis*- and *trans*-2,5-dimethyl-THF); 4.77 (d, J_{cis} = 10 Hz, =CHH); 4.85 (d, J_{trans} = 17 Hz, =CHH); δ 5.79 (br s, partially obscured by resonance of excess diene, CH=CH₂); resonance for YCH₂CH₂CH₂ obscured by Cp* resonance.

Acknowledgment. Financial support from the National Science Foundation (CHE-9972183) is gratefully acknowledged. Grants from the NSF (CHE-9629688) and NIH (I S10 RR04981-01) for the purchase of the NMR spectrometers are acknowledged. We thank Dr. Ting-Yu Lee for helpful discussions.

Supporting Information Available: General procedures; experimental information for compounds **1**, **6–9**, **12–14**, and **18**; data tables and van't Hoff plots for temperature-dependent NMR spectra of equilibrium mixtures of **6** and **10**, **7** and **11**, and **8** and **12**; temperature-dependent ¹H NMR spectra for **1**, **6**, equilibrium mixtures of **1** and **13**, **6** and **10**, **7** and **11**, and **8** and **12**; temperature-dependent ¹³C NMR spectra of **7** and **8**; Δ*G* and Δ*H* diagrams for **1**, **6**, **7**, and **8** (PDF). This material is available free of charge via the Internet at <http://pubs.acs.org>.

JA9931022